JACS
JOURNAL OF THE AMERICAN CHEMICAL SOCIETY
Communication
pubs.acs.org/JACS

Metal–Alane Adducts with Zero-Valent Nickel, Cobalt, and Iron

P. Alex Rudd, Shengsi Liu, Laura Gagliardi, Victor G. Young, Jr., and Connie C. Lu*

Department of Chemistry and Supercomputing Institute, University of Minnesota, 207 Pleasant Street SE, Minneapolis, Minnesota 55455, United States

Supporting Information

ABSTRACT: Coordination complexes that pair a zero-valent transition metal (Ni, Co, Fe) and an aluminum(III) center have been prepared. They add to the few examples of structurally characterized metal alanes and are the first reported metallalumatranes. To understand the M–Al interaction and gauge the effect of varying the late metal, the complexes were characterized by X-ray crystallography, electrochemistry, UV–Vis–NIR and NMR spectroscopies, and theoretical calculations. The M–Al bond strength decreases with varying M in the order Ni > Co > Fe.

The adsorption of late transition metals on an oxide support forms the basis of many heterogeneous catalysts. The catalytic activity and selectivity are both highly dependent on the choice of the metal, the choice of the oxide, and the extent of metal–support interaction. Notably, strong metal–support bonds have been proposed as the cause of enhanced catalyst performance as well as surface deactivation.[1] Research efforts remain focused on understanding the structure–activity relationships of these metal–support interactions.[2]

Dinuclear metal–alane coordination complexes are the simplest representations of the interface of late transition metals adsorbed on alumina.[3] A systematic study of the metal–alane bonding for a wide range of late transition metals and oxides may provide crucial insights for catalyst design. Despite the plethora of metal–borane complexes,[4] the corresponding metal–alane complexes are unusual. The few structurally characterized examples are shown in Figure 1.[5]

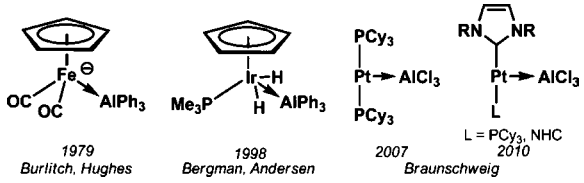

Figure 1. Structurally characterized metal–alane adducts.

Bonds between transition metals and group 13 metals are fundamentally interesting because of the potential reversal of the metal and ligand roles in the M→L dative bond: the metal acts as the Lewis base, donating its electron density to the Lewis acidic group 13 ion.[6] Incorporating the borane unit into the ligand is an effective strategy for stabilizing metallaboratranes.[7] The ligand arms bridge the metal center and the boron atom, serving as auxiliary supports for the M→B bond. Bourissou and co-workers have used these ligand "buttresses" to stabilize Au→Ga, Pd→In, and Au→In bonds,[8] but the corresponding Au→Al species was unstable and rearranged to a nonbonding $Au^{+}Al^{-}$ zwitterion.[9] Building on this strategy, we report the first examples of metallalumatrane complexes. The M→Al interactions are compared for M = Ni^0, Co^0, and Fe^0.

To facilitate the synthesis of metallalumatranes, we introduce the dinucleating heptadentate ligand **1** (Scheme 1). To generate **1**, the key step is the triple dehydration reaction of $N(o\text{-}NH_2C_6H_4)_3$[10] with 3 equiv of diisopropylphosphinomethanol. In the next step, **1** is triply deprotonated and reacted with $AlCl_3$ to obtain the alumatrane–phosphine complex **2** (abbreviated as AltraPhos) as a white powder.[11] AltraPhos is characterized by a singlet at 8.5 ppm in the ^{31}P NMR spectrum, which is slightly shifted from the 3.0 ppm peak for **1** (in C_6D_6). In the ^{1}H NMR spectrum of **2**, only one resonance per proton type was observed, suggesting threefold symmetry. Further structural information was provided by an X-ray diffraction (XRD) study of a single crystal of **2** grown from acetonitrile. The solid-state structure reveals a trigonal-bipyramidal aluminum center with a bound CH_3CN molecule in the apical pocket and dangling phosphine arms (Scheme 1 inset).

With its available phosphine donors, AltraPhos readily coordinates a variety of late transition metals. Reaction of **2**

Scheme 1. Syntheses of Proligand 1, AltraPhos (2) and the Metallalumatrane Coordination Complexes and Structure of 2

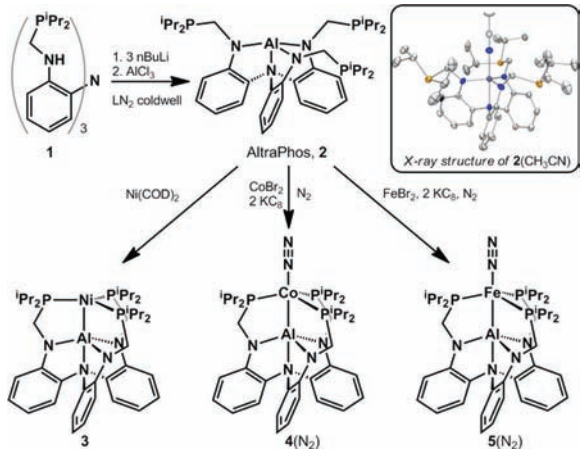

Received: October 23, 2011
Published: November 28, 2011

   dx.doi.org/10.1021/ja2099744 | J. Am. Chem.Soc. 2011, 133, 20724–20727

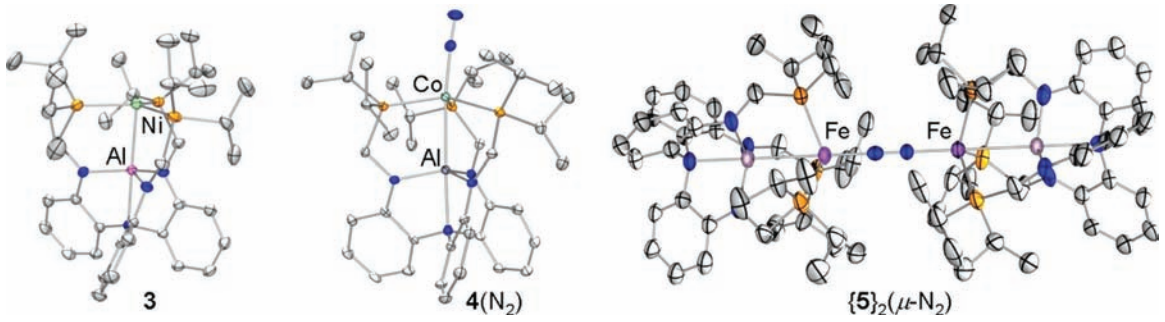

Figure 2. Solid-state structures of **3**, **4**(N_2), and {**5**}$_2$(μ-N_2) shown at the 50% probability level. H atoms and noncoordinating solvent molecules have been omitted for clarity.

with Ni(COD)$_2$ (COD = 1,5-cyclooctadiene) yields the formally zero-valent nickel–alane complex **3**. As expected for a (Ni–Al)[10] d-electron count, **3** is diamagnetic. The coordination of all three phosphine arms is consistent with the observations of a single peak at 49.4 ppm in the ^{31}P NMR spectrum and of diastereotopic methylene protons in the ^{1}H NMR spectrum. The broad singlet in the ^{27}Al NMR spectrum is shifted slightly upfield from 82.2 ppm in AltraPhos to 78.6 ppm in **3**, suggesting some gain in electron density at the aluminum center, presumably via a Ni→Al dative bond.

Further evidence for Ni–Al bonding in **3** was found by analysis of its solid-state structure (Figure 2). The Ni–Al bond distance of 2.450(1) Å is identical to the sum of the Ni and Al covalent radii.[12] The Al–N_{apical} bond increases from 2.060(3) Å in AltraPhos to 2.099(2) Å in **3**: one interpretation is that the Ni→Al interaction occurs at some cost to the N_{apical}→Al dative bond.

AltraPhos was found to stabilize other zero-valent transition metal centers, namely, Co and Fe, upon mixing of **2**, the corresponding metal dibromide, and 2 equiv of the reductant KC_8. Both products are paramagnetic (^{1}H NMR), and the IR spectra of their solid samples (KBr pellets) contain a single N–N stretching frequency: 2081 cm^{-1} for the Co complex **4**(N_2) and 2010 cm^{-1} for the Fe complex **5**(N_2) [in free N_2(g), ν_{NN} = 2331 cm^{-1}].[13] The IR data are consistent with end-on coordination of the N_2 molecule at the metal center, as represented by M(N_2)(AltraPhos). The effect of exchanging Co^0 for Fe^0 is to lower the N–N stretching frequency by 71 cm^{-1}. A similar trend was observed in another system wherein Fe(N_2) and Co(N_2) species are available. Specifically, Peters and co-workers reported a difference of ∼55 cm^{-1} for Fe^{I}(N_2) and Co^{I}(N_2) complexes supported by tris(phosphino)silyl ligands.[14] Moret and Peters also reported an analogous B← Fe^0(N_2) complex with the tris(phosphino)borane (TPB) ligand.[15] The N–N stretching frequency of this complex is 2011 cm^{-1}, nearly identical to that of **5**(N_2). The N_2 ligand in the B←Fe^0(N_2) complex was reported to be labile, which impeded crystallographic characterization.

XRD studies confirmed the end-on monometallic nature of the cobalt complex, Co(N_2)(AltraPhos) [**4**(N_2)], but revealed an end-on N_2-bridged diiron complex, {Fe(AltraPhos)}$_2$(μ-N_2) [{**5**}$_2$(μ-N_2)] (Figure 2). In the Co complex, the N–N bond distance of 1.107(4) Å is slightly elongated relative to that in free N_2(g) (1.0975 Å).[13] In the Fe structure, the N–N bond distance is 1.146(7) Å; the significantly greater activation of the N_2 ligand is partly attributed to the end-on bridged versus end-on unbridged mode.[16] The observation of both **5**(N_2) and {**5**}$_2$(μ-N_2) suggests that an equilibrium exists between these two species and establishes that N_2 is indeed a labile ligand.

Whether an M–Al interaction exists is not obvious, as the two nuclei are forced into proximity by the ligand scaffold. The ratios of the M–Al bond distances to their respective covalent radii (r) are all near unity (Table 1), arguing for an M–Al interaction in all three complexes.[6a] On the basis of the opposite trend for r, the strength of the M–Al interaction decreases in the order Ni–Al > (N_2)Co–Al > (μ-N_2)Fe–Al. Also, the apical N–Al bond length increases in going from AltraPhos to **3** (M = Ni) to **4**(N_2) (M = Co) and {**5**}$_2$(μ-N_2) (M = Fe). The lengthening of the Al–N_{apical} bond correlates with the distortion of the transition-metal center from the ideal trigonal-bipyramidal geometry to a pseudotetrahedral geometry. The sums of the P–M–P angles are 349.5° in **4**(N_2) and 335.0° in {**5**}$_2$(μ-N_2), indicating significant deviations from planarity. Moret and Peters previously described a very weak Fe–B interaction in the ferraboratrane imide complex (TPB)-Fe≡NPh based on the long Fe···B bond distance (r = 1.21) and the nearly tetrahedral coordination geometry of the iron center ($\sum$P–Fe–P = 333.0°).

Table 1. Geometrical Parameters, Including Bond Lengths (Å) and Angles (deg), for 2(CH$_3$CN), 3, 4(N_2), and {5}$_2$(μ-N_2)[a]

	2(CH$_3$CN)	3	4(N_2)	{5}$_2$(μ-N_2)
M		Ni	Co	Fe
M–Al	—	2.450(1)	2.6202(9)	2.809(2)
r^b	—	1.00	1.06	1.11
Al–N_{apical}	2.060(3)	2.099(2)	2.187(2)	2.176(4)
N–N	—	—	1.107(4)	1.146(7)
$\sum$P–M–P	—	359.02(6)	349.47(5)	335.03(3)
$\sum N_{eq}$–Al–N_{eq}	356.58(3)	354.5(1)	351.5(2)	351.56(9)

[a]Estimated standard deviations are given in parentheses. [b]Ratio of the M–Al bond length to the sum of the l.s. M and Al covalent radii.[12]

Distortions from threefold symmetry are most notable in the solid-state structure of Co **4**(N_2). The Co–P bond lengths are different [2.2408, 2.2712, and 2.2859(9) Å] as are the P–Co–P angles [105.07, 111.90, and 132.50(3)°]. In contrast, the M–P bond lengths in **3** and in {**5**}$_2$(μ-N_2) are within 0.015 Å, and their P–M–P angles differ by less than 1°. A simple explanation is that the (Co–Al)[9] d-electron count induces a Jahn–Teller distortion from C_3 symmetry (see below). Consistent with this conjecture, the (Ni–Al)[10] and (Fe–Al)[8] configurations are expected to retain C_3 symmetry.

To investigate the effects of the M–Al interaction on the late transition metal, electrochemical studies of compounds **3**,

dx.doi.org/10.1021/ja2099744 | J. Am. Chem.Soc. 2011, 133, 20724–20727

$4(N_2)$, and $5(N_2)$ were conducted. The cyclic voltammograms of the metal complexes each display only one reversible wave (Figure 3). In the case of **3**, the reversible oxidation at −0.74 V

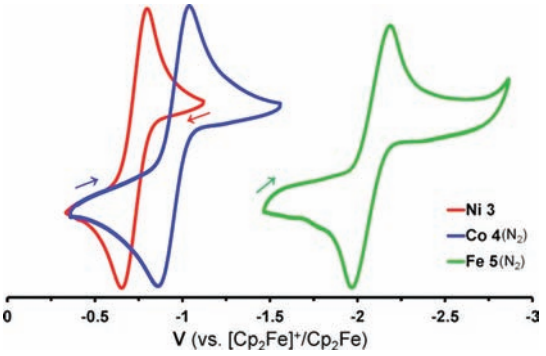

Figure 3. Cyclic voltammograms of **3**, $4(N_2)$, and $5(N_2)$ in 0.1 M $[nBu_4N]PF_6$/THF at 50 mV/s. Only reversible waves are shown.

vs Fc^+/Fc is assigned to the Ni^0/Ni^I redox couple. No reduction events are seen. In contrast, $4(N_2)$ and $5(N_2)$ exhibit single reversible reductions at −0.95 and −2.08 V, respectively, which are assigned as the formal M^{-I}/M^0 couples. The effect of swapping Co for Fe results in a dramatic 1.12 V difference in the M^{-I}/M^0 redox potentials, with Co being easier to reduce than Fe. The Fe^{-I}/Fe^0 potential of **5** is quite near the value of −2.19 V reported for (TPB)Fe(N_2).[15] The similarity is consistent with the two complexes having nearly identical N−N stretching frequencies. Their similarities also indicate that Fe^0−Al^{III} and Fe^0−B^{III} interactions must be very weak and that the formal exchange of Al for B has little to no effect on the iron center in this instance.

The M−Al interaction in this series was also interrogated with UV−Vis−NIR spectroscopy (Figure 4 top). Common to all of the complexes is a band with $\lambda_{max} \approx 340$ nm, which is assigned to the $\pi \rightarrow \pi^*$ transition of the ligand backbone. While AltraPhos has no signal beyond 380 nm, the rest of the complexes have absorptions in the visible and/or NIR regions. **3** has three visible peaks with λ_{max} = 430, 490, and 600 nm. $4(N_2)$ and $5(N_2)$ have NIR bands at 1400 and 890 nm, respectively, though the former is weak (ε < 100 L mol^{-1} cm^{-1}). In the visible region, $4(N_2)$ has a few relatively weak bands, whereas $5(N_2)$ has an intense absorption with λ_{max} = 411 nm. The nature of these transitions was elucidated with time-dependent density functional theory (TD-DFT) calculations (see below).

We conducted DFT studies to obtain a better understanding of the M−Al electronic structures beyond the general $(M-Al)^n$ descriptor. The DFT-optimized geometries of **3**, $4(N_2)$, and $5(N_2)$ corresponded to the experimental structures well when the Al and M atoms were treated with SDD and SDD+2f pseudopotential basis sets, respectively [6-311+G(2df,p) for P and N and 6-31G(d) for C and H atoms; M06-L;[17] Gaussian 09].

In all cases, open-shell calculations were employed, and no spin density (i.e., radical character) was found on any ligand atoms, including Al and N_2. The qualitative correlation diagram based on the calculations is shown in Figure 5. As expected, the $d_{xy}/d_{x^2-y^2}$ and d_{xz}/d_{yz} pairs are degenerate for $(Ni-Al)^{10}$ and $(Fe-Al)^8$, whereas the d_{xy} and $d_{x^2-y^2}$ orbitals are nondegenerate for $(Co-Al)^9$. For **3**, the lowest unoccupied molecular orbital (LUMO) is primarily a Ni $4p_z$ orbital.

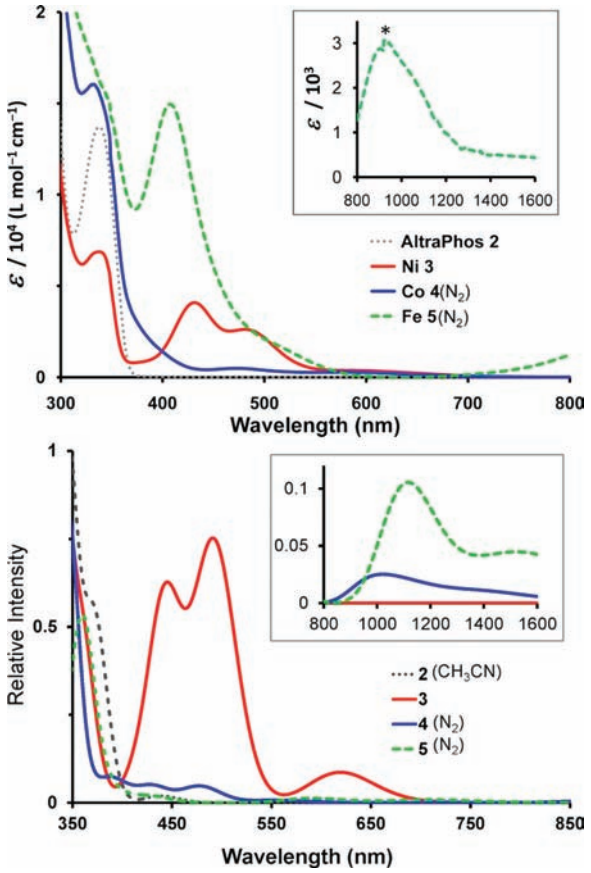

Figure 4. (top) UV−vis spectra of **2**, **3**, $4(N_2)$, and $5(N_2)$ in THF at room temperature. Inset: NIR spectrum of $5(N_2)$ (* denotes the swapping of light sources). (bottom) TD-DFT-predicted UV−vis−NIR spectra of $2(CH_3CN)$, **3**, $4(N_2)$, and $5(N_2)$. The inset shows the NIR region.

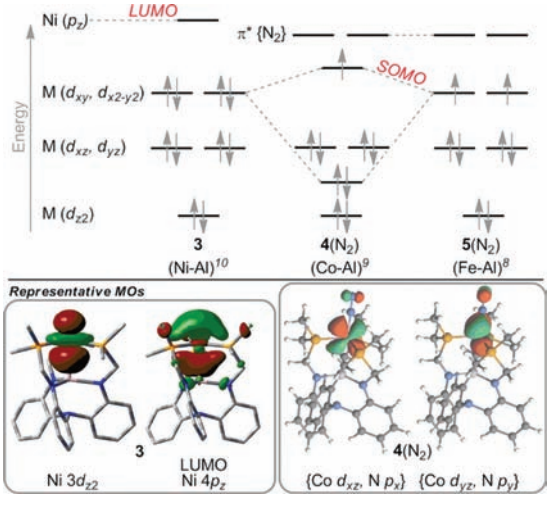

Figure 5. Qualitative correlation diagram for the d-orbital manifold and the LUMOs for **3**, $4(N_2)$, and $5(N_2)$. MO energies are not drawn to scale.

TD-DFT calculations (B3LYP, ORCA 2.7.0b) with solvent considerations (COSMO) were also performed to predict the electronic absorption spectra (Figure 4 bottom). The general agreement between the calculated and experimental spectra is good. Ligand-to-ligand charge-transfer (LLCT) transitions occur in the UV range, and in all three metal complexes,

dx.doi.org/10.1021/ja2099744 | J. Am. Chem.Soc. 2011, 133, 20724−20727

intense π-based LLCT bands are seen between 325 and 360 nm (exptl ~340). For **3**, three distinct bands are predicted in the visible range at λ_{max} = 440, 490, and 620 nm, in excellent agreement with the experimental spectrum of **3**. These transitions are assigned as follows: 440 nm, d_{xz}/d_{yz} to $4p_z$ (LUMO); 490 nm, (d_{z^2} + Lπ) to $4p_z$; 620 nm, $d_{xy}/d_{x^2-y^2}$ to $4p_z$. The more pure d_{z^2} to $4p_z$ transition is predicted at 360 nm, appearing as a shoulder on the LLCT band in Figure 4. Because several transitions involve the LUMO, the ligand-field energies can be extracted: $\Delta(d_{z^2}, d_{xz}/d_{yz})$ = 0.66 eV; $\Delta(d_{xz}/d_{yz}, d_{xy}/d_{x^2-y^2})$ = 0.79 eV; $\Delta(d_{xy}/d_{x^2-y^2}, 4p_z)$ = 2.0 eV.

Although the TD-DFT results for Co complex **4**(N_2) and Fe complex **5**(N_2) are complicated by MO mixing in the ground and excited states, some important information can be gleaned. Excitations to the metal p_z orbital occur near 300 nm (see the Supporting Information for details). Far-visible bands arising from metal d → $\pi^*(N_2)$ transitions occur at 400 and 431 nm for **4**(N_2) and 362 nm for **5**(N_2). Additional d_{z^2}(Fe) → $\pi^*(N_2)$ peaks are red-shifted to 432 and 434 nm. Metal d−d transitions into the singly occupied MO (SOMO) account for the remaining bands at 557, 990, and 1133 nm for **4**(N_2) and at 592 and 1113 nm for **5**(N_2). There are two noteworthy discrepancies between the calculated and experimental spectra. The NIR bands for Co are predicted to have similar intensities as the visible bands, yet experimentally only a very weak signal is observed at 1400 nm (ε < 100 L mol^{-1} cm^{-1}). More troubling, the far-visible bands for **5**(N_2) are predicted to have relatively low intensity, but experimentally, the 411 nm band is remarkably intense ($\varepsilon = 1.5 \times 10^4$ L mol^{-1} cm^{-1}). In the case of the Fe complex, we have made the simplifying assumption that the N_2-bridged species {**5**}$_2$(μ-N_2) is a minor species in solution relative to **5**(N_2). If this is not the case, then additional transitions are expected for {**5**}$_2$(μ-N_2), and they could possibly account for the intense band at 411 nm. The solution equilibrium between **5**(N_2) and {**5**}$_2$(μ-N_2) is currently under study.

While we have varied the late metal to probe the chemical nature of M→Al bonds, another intriguing and complementary study would be to probe the effect of the supporting center on an invariant late metal center. Future efforts are focused on using the dinucleating proligand **1** to access novel chemical bonds between two main-group and/or transition-metal elements.

■ ASSOCIATED CONTENT

Ⓢ Supporting Information

Experimental procedures, X-ray crystallographic data (CIF), computational details, and physical data. This material is available free of charge via the Internet at http://pubs.acs.org.

■ AUTHOR INFORMATION

Corresponding Author

clu@umn.edu

■ ACKNOWLEDGMENTS

Aubrey (Sperier) Arenivas and Abbas Mulla are acknowledged for their preliminary experimental and computational contributions, respectively. S.L. thanks Zahid Ertem for computational advice. We thank Professor Dave Blank for the generous use of his Vis−NIR spectrophotometer. Computing support and resources were provided by the Minnesota Supercomputing Institute. Dr. Letitia Yao assisted with the NMR spectroscopic studies. This work was made possible by support from the University of Minnesota. Acknowledgment is made to the donors of the ACS Petroleum Research Fund (Grant 50395-DNI3 to C.C.L.) and to the U.S. DOE (Grant DE-SC002183 to L.G.) for partial support of this research.

■ REFERENCES

(1) (a) Tauster, S. J.; Fung, S. C.; Baker, R. T. K.; Horsley, J. A. *Science* **1981**, *211*, 1121. (b) Tsakoumis, N. E.; Rønning, M.; Borg, Ø.; Rytter, E.; Holmen, A. *Catal. Today* **2010**, *154*, 162.

(2) (a) Farmer, J. A.; Campbell, C. T. *Science* **2010**, *329*, 933. (b) Kwak, J. H.; Hu, J.; Mei, D.; Yi, C.-W.; Kim, D. H.; Peden, C. H. F.; Allard, L. F.; Szanyi, J. *Science* **2009**, *325*, 1670.

(3) Studies proposing metal−support interactions between metal and aluminum centers: (a) Venezia, A. M.; Bertoncello, R.; Deganello, G. *Surf. Interface Anal.* **1995**, *23*, 239. (b) Kunimori, K.; Ikeda, Y.; Soma, M.; Uchijima, T. *J. Catal.* **1983**, *79*, 185. (c) Bhatia, S.; Bakhshi, N. N.; Mathews, J. F. *Can. J. Chem. Eng.* **1978**, *56*, 575.

(4) (a) Braunschweig, H.; Dewhurst, R. D.; Schneider, A. *Chem. Rev.* **2010**, *110*, 3924. (b) Braunschweig, H.; Dewhurst, R. D. *Dalton Trans.* **2011**, *40*, 549.

(5) (a) Burlitch, J. M.; Leonowicz, M. E.; Petersen, R. B.; Hughes, R. E. *Inorg. Chem.* **1979**, *18*, 1097. (b) Golden, J. T.; Peterson, T. H.; Holland, P. L.; Bergman, R. G.; Andersen, R. A. *J. Am. Chem. Soc.* **1998**, *120*, 223. (c) Braunschweig, H.; Gruss, K.; Radacki, K. *Angew. Chem., Int. Ed.* **2007**, *46*, 7782. (d) Bauer, J.; Braunschweig, H.; Brenner, P.; Kraft, K.; Radacki, K.; Schwab, K. *Chem.—Eur. J.* **2010**, *16*, 11985.

(6) (a) Amgoune, A.; Bourissou, D. *Chem. Commun.* **2011**, *47*, 859. (b) Parkin, G. *Organometallics* **2006**, *25*, 4744. (c) Hill, A. F. *Organometallics* **2006**, *25*, 4741.

(7) (a) Hill, A. F.; Owen, G. R.; White, A. J. P.; Williams, D. J. *Angew. Chem., Int. Ed.* **1999**, *38*, 2759. (b) Mihalcik, D. J.; White, J. L.; Tanski, J. M.; Zakharov, L. N.; Yap, G. P. A.; Incarvito, C. D.; Rheingold, A. L.; Rabinovich, D. *Dalton Trans.* **2004**, 1626. (c) Pang, K.; Tanski, J. M.; Parkin, G. *Chem. Commun.* **2008**, 1008. (d) Bontemps, S.; Bouhadir, G.; Gu, W.; Mercy, M.; Chen, C.-H.; Foxman, B. M.; Maron, L.; Ozerov, O. V.; Bourissou, D. *Angew. Chem.* **2008**, *47*, 1503. (e) Sircoglou, M.; Bontemps, S. b.; Bouhadir, G.; Saffon, N.; Miqueu, K.; Gu, W.; Mercy, M.; Chen, C.-H.; Foxman, B. M.; Maron, L.; Ozerov, O. V.; Bourissou, D. *J. Am. Chem. Soc.* **2008**, *130*, 16729.

(8) (a) Sircoglou, M.; Mercy, M.; Saffon, N.; Coppel, Y.; Bouhadir, G.; Maron, L.; Bourissou, D. *Angew. Chem., Int. Ed.* **2009**, *48*, 3454. (b) Derrah, E. J.; Sircoglou, M.; Mercy, M.; Ladeira, S.; Bouhadir, G.; Miqueu, K.; Maron, L.; Bourissou, D. *Organometallics* **2011**, *30*, 657.

(9) Sircoglou, M.; Bouhadir, G.; Saffon, N.; Miqueu, K.; Bourissou, D. *Organometallics* **2008**, *27*, 1675.

(10) Jones, M. B.; MacBeth, C. E. *Inorg. Chem.* **2007**, *46*, 8117.

(11) Su, W.; Kim, Y.; Ellern, A.; Guzei, I. A.; Verkade, J. G. *J. Am. Chem. Soc.* **2006**, *128*, 13727.

(12) Cordero, B.; Gomez, V.; Platero-Prats, A. E.; Reves, M.; Echeverria, J.; Cremades, E.; Barragan, F.; Alvarez, S. *Dalton Trans.* **2008**, 2832.

(13) MacKay, B. A.; Fryzuk, M. D. *Chem. Rev.* **2004**, *104*, 385.

(14) Whited, M. T.; Mankad, N. P.; Lee, Y.; Oblad, P. F.; Peters, J. C. *Inorg. Chem.* **2009**, *48*, 2507.

(15) Moret, M.-E.; Peters, J. C. *Angew. Chem., Int. Ed.* **2011**, *50*, 2063.

(16) Fryzuk, M. D.; Haddad, T. S.; Mylvaganam, M.; McConville, D. H.; Rettig, S. J. *J. Am. Chem. Soc.* **1993**, *115*, 2782.

(17) (a) Zhao, Y.; Truhlar, D. G. *Acc. Chem. Res.* **2008**, *41*, 157. (b) Zhao, Y.; Truhlar, D. G. *J. Chem. Phys.* **2006**, *125*, No. 194101.